Article

Reduction of DC-drift in $LiNbO_3$-based electro-optical modulator

Aleksei Sosunov [1]*, Roman Ponomarev [1,2], Anton Zhuravlev [1], Sergey Mushinsky [1] and Mariana Kuneva [3]

[1] Department of Physics, Perm State University, 614068, Perm, Russia; avsosunov@psu.ru
[2] Perm Federal Research Center, Ural Branch of Russian Academy of Science, 614990, Perm, Russia; Lenina Str. 15A, rsponomarev@psu.ru
[3] Institute of Solid State Physics Bulgarian Academy of Sciences, Tzarigradsko Chaussee 72, Blvd., 1784 Sofia, Bulgaria; kuneva@issp.bas.bg
* Correspondence: avsosunov@psu.ru; Tel.: (+7-342-2396-410)

Abstract: This work involves results of research on short-term and long-term DC-drifts in electro-optical modulators based on annealed proton exchange waveguides in $LiNbO_3$ crystals after wafer pre-annealing. The relaxation time of the DC-drift of the operating point for a short-term drift is minutes, and for a long-term drift, hours and days. DC-drift was measured by applying bias voltage and changing crystal temperature. Obtained results shows significant impact on stability of operating point in EO-modulators after treatment of defective structure of the near-surface layer of a $LiNbO_3$ crystal. Treatment of the disturbed near-surface layer of a $LiNbO_3$ crystal results in twice reduction of short-term DC-drift and increase of operation stability of electro-optical modulators during long-term measurement of temperature by activation energy calculation.

Keywords: lithium niobate, electro-optical modulator, DC-drift, operating point

1. Introduction

Electro-optical (EO)-modulators based on lithium niobate ($LiNbO_3$) are described in detail in research literature as effective broadband devices with low optical losses. These EO-modulators are widely used in telecommunication systems with high data transmission speed, optical fiber gyroscopes and sensors requiring external signal modulation [1].

Despite significant improvement in development of $LiNbO_3$ optical integrated circuits [2,3], until now no clear solution has been found for one of the major challenges – stabilization of an EO-modulator operating point when modulators operate over a long period of time as part of data transmission systems.

Transfer function of an EO-modulator output optical power P_{out} and voltage V applied to modulator electrodes is:

$$P_{out}(V,t,T) = \frac{L_{in}P_{in}}{2}\left(1 + cos\left[\frac{\pi V}{V_\pi} + \Phi_0(t,T)\right]\right) \quad (1)$$

where L_{in} – inserted optical losses, P_{in} – optical input power, t – time, T – temperature, Φ_0 – phase shift, V_π – half-wave voltage or voltage required to change from maximum power to minimum power which is determined as follows:

$$V_\pi = \frac{\lambda \cdot d}{\gamma L \cdot n_{eff}^3 r_{eff}}, \quad (2)$$

where γ – overlap integral of electric field and waveguides, λ – wavelength, L – length of a waveguides active part, d – distance between electrodes, n_{eff} – effective refractive index of a waveguides, r_{eff} – effective electro-optical coefficient depending on material, optical polarization and electrode design [4].

The transfer function is nonlinear and depends on device design parameters – L, d, λ, as well as on material parameters of the crystal and waveguides – r_{eff} and n_{eff}. Design parameters are constant values or are strictly controlled during modulator operation. Material parameters depend on temperature, photorefraction effects, pyro- and piezoelectric effect in a crystal and strain. This dependency is rather complex, it has a clear character and can be considered when designing and operating modulators. However

Preprints (www.preprints.org) | NOT PEER-REVIEWED | Posted: 15 November 2021 doi:10.20944/preprints202111.0262.v1

long-term studies of EO-modulators show that their operating point can drift at constant temperature and with external voltage applied [5, 6]. This is related to drift of moving charged defects in a lattice and not well understood.

Many modern papers [7-13] study the increase in stability of an operating point of EO-modulators by improving design and methods of device encapsulation. Comparison analysis of key methods of increasing the stability of an operating point of EO-modulators is given in [14]. However the paper [15] shows that major cause of drifting operating point is relaxation of electric charges resulting from structural irregularity of $LiNbO_3$ crystal and inhomogeneous electric properties (conductivity). When voltage is applied, these electric irregularities lead to redistribution of electric charges resulting in time-dependent depolarizing electric field. Thus these are material parameters, rather than design or assembly method that contribute the most to instability of EO-modulators.

This conclusion may seem obvious at first sight, but studies of constant (internal) drift (DC-drift) processes neglected material parameters of a crystal, specifically, its composition, structure and properties of surface layer which contains a waveguides, as well as density of dislocations in this layer and diffusion coefficients of point defects.

We studied the microstructure of surface layer of a $LiNbO_3$ crystal and demonstrated that this layer has an irregular structure with fragmentation components [16]. These changes of the $LiNbO_3$ crystal structure should be considered from the microscopic point of view as increase in the number of point defects and dislocations in the area of annealed proton exchange (APE) waveguides which is important for stability of EO-modulators. The recent study [17] has confirmed that changed ratio [Li]/[Nb] can indicate that near-surface layer of $LiNbO_3$ crystal contains more complex forms of structural irregularities, e.g. light diffusion paths represented by dislocation grids. Then we offered [18] an approach to treatment a disturbed near-surface layer of a $LiNbO_3$ crystal to increase its structural homogeneity and stability of operating point in EO-modulators.

This work is a next step which studies the behavior of EO-modulators based on annealed proton exchange waveguides contained in $LiNbO_3$ crystals after treatment crystal structure. The purpose of this research is to analyze the impact of the surface structure of a $LiNbO_3$ crystal on stability of optical parameters of EO-modulators.

2. Materials and Methods

2.1. Sample preparation

EO-modulators were prepared from congruent $LiNbO_3$ X-cut (manufactured by Crystal Technology Inc). One of the $LiNbO_3$ wafers was pre-annealed (hereinafter referred to as treatment) at 500 °C for 3 hours and then cooled down slowly with furnace designed to treatment the structure of disturbed surface layer as described in [18]. This temperature is ideal for obtaining a more homogeneous structure of near-surface layer of a $LiNbO_3$ crystal and $H_xLi_{1-x}NbO_3$ optical waveguides. Treatment of $LiNbO_3$ directly affects the optical characteristics of APE channel waveguides with identical formation technology. In particular, defects and internal stresses in the near-surface layer of $LiNbO_3$ can increase the light scattering passing through optical channel waveguides. Moreover, any defects in the region of the waveguides obtained by ion exchange methods deteriorate the polarizing properties of the waveguide, which leads to decrease in the extinction of the EO-modulator.

APE waveguides were created using direct photolithography. For a protective film we used Al_2O_3 layer (300 nm) deposited by electron beam evaporation. Then we deposited a positive-acting photoresist (1 um). After drying and development of the photoresist, its active part was removed in organic solvent. Then, Al_2O_3 protective film was etched using nitric acid solution and removed remains of photoresist. 6 um wide channels were created.

Proton exchange took place in a closed zirconium reactor at 170 °C for 2 hours followed by cooling at 10 °C/min. Annealing was performed at 350 °C for 5.5 hours followed by cooling in an oven.

Preprints (www.preprints.org) | NOT PEER-REVIEWED | Posted: 15 November 2021 doi:10.20944/preprints202111.0262.v1

At the next step, we deposited a 0.5 um layer of gold on a $LiNbO_3$ support surface by vacuum evaporation. To make the final structure of electrodes, we also used the process of photolithography and chemical treatment. A couple of samples with optical waveguides and electrodes on their surfaces were cut into 15 mm wide blocks. As a result we have obtained a couple of chips with treatment $LiNbO_3$ structure and a couple of standard chips which remained unchanged. All chips were obtained at identical process parameters. At the last step we connected the chips to optical fiber using a NanoMax 311 micromovements system and a machine vision system (Fig. 1).

After this the samples were treated in isopropyl alcohol and de-ionized water for 10 minutes at each step of producing EO-modulator components.

Speaking of the above processes of creating integral components on the $LiNbO_3$ surface, only proton exchange contributes to changes of the crystal structure rather than related secondary physical and chemical processes, specifically:

- Maximum crystal heating temperature (350 °C) is significantly lower than the temperature when the crystal composition starts to change (above 600 °C), while pyroelectric effect is characteristic of the crystal Z-cut where Li^+ ions are redistributed next to two polar faces. These processes are not characteristic of the $LiNbO_3$ X-cut, because the direction of the normal line to the crystal X-cut is nonpolar. Considering strong connections between oxygen base and Nb^{+5} ions, it is fair to say that the crystal composition does not change in areas where it is not subject to proton exchange when creating waveguides by described methods;
- Time of photoresist treatment is selected in such a way as to avoid interaction between acid and support structure. As far as the development process is concerned, $LiNbO_3$ is inert to organic developers;
- UV exposure during connection of the chips and fiber can result in generation of free electrons in $LiNbO_3$ after photovoltaic effect, but their relaxation time is much less than the time between assembly and testing of the samples.

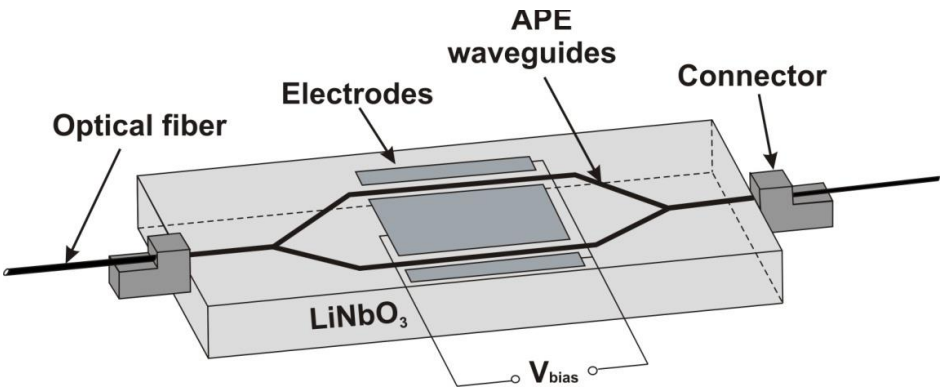

Figure 1. Schematic of EO-modulator.

2.2. Optical losses

Losses per cm in $LiNbO_3$ crystal were measured on a slope of a back-reflection curve using a Luna OBR-5T-50 reflection meter. The spatial resolution enables to take measurements every 30 um on a homogeneous linear section within the topology of EO-modulator.

Optical losses were calculated for a wavelength of 1.55 um by measuring output power of source radiation and after radiation distribution between waveguides of an EO-modulator (fiber-to-fiber). To measure optical power, we used Santec PEM-330 optical power meter.

2.3. Drift of operating point depending on voltage applied V_{bias}

We tested short-term drift of an operating point in EO-modulators by applying DC voltage to modulator electrodes and recording changes of the output optical power. Without drift output optical power should stabilize immediately after voltage is applied to electrodes. However the measurement P_{out} was changing during a certain period after

Preprints (www.preprints.org) | NOT PEER-REVIEWED | Posted: 15 November 2021 doi:10.20944/preprints202111.0262.v1

the voltage was applied. The most interesting results were obtained at hopping changes of the sign of applied voltage. All experiments were performed in the voltage range of ±8 *V* at an increment of 1 *V* and holding time of 5 minutes after the sign of applied voltage changes. We used battery like low noise chemical voltage source. The voltage using a continuous adjusting resistor manually was changed. After that, the polarity at a fixed voltage was changed to study the short-term drift. Based on obtained results we analyzed the relaxation time of operating point of EO-modulators and recovered the transfer function. The lighting source was a highly stable narrow-band laser with a wavelength of 1.55 um and power of 3 mW. For a layout of the experiment device see Fig. 2.

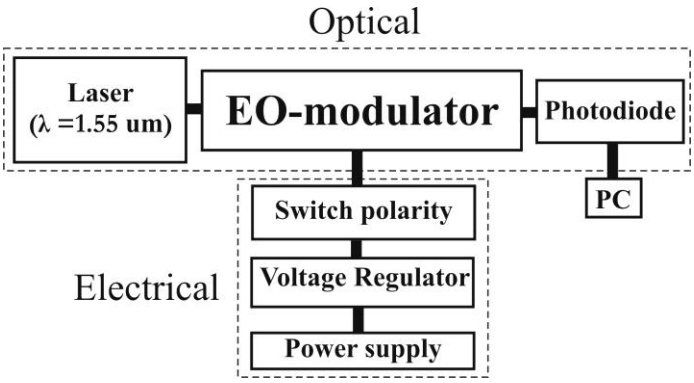

Figure 2. Schematic of DC-drift measurements.

2.4. Drift of operating point depending on temperature

Temperature measurements were performed to calculate activation energy of DC-drift of operating point of EO-modulators. Understanding activation processes in $LiNbO_3$ near-surface layer in the area of APE channel waveguides and electrodes at temperature effect will enable us to evaluate the effectiveness of $LiNbO_3$ structure treatment and its impact on drift of operating point in EO-modulators. First, we fixed the operating point at a constant voltage of 4.5 V which corresponds to a linear section of the transfer function for all test samples for a wavelength λ = 1.55 um. Then test samples were put in a heater and heated to 25, 50, 70 and 90 °C with holding time of 7 hours (temperature range did not exceed 100 °C according to the manufacturer's recommendation). Before changing the temperature the samples had to cool down for 12 hours. After this we measured the change of output optical power corresponding to the drift of operating point of EO-modulators.

3. Results and Discussion

3.1. Short-term DC-drift

Before testing the stability of DC-drift based on treatment near-surface layer of $LiNbO_3$ crystal in EO-modulators we measured optical losses both in a chip by an optical reflectometry and in the entire modulator by a fiber-to fiber method. Table 1 shows measured optical losses of the test samples. It is known that optical losses per unit length of stable APE waveguides in a $LiNbO_3$ crystal are ~ 0.15 dB/cm [19]. The tests resulted in stable APE waveguides with standard characteristics. The spread of loss values per unit length in chips is determined by measurement errors, while the highest optical losses in modulators occur at the connection point of a chip and optical fiber.

Table 1. Optical losses and half-wave voltage

Characteristic	APE
Waveguide loss, dB/cm	0.13-0.17
Average fiber-to-fiber loss, dB	6.5
Half-wave voltage, V	3.5-6

Preprints (www.preprints.org) | NOT PEER-REVIEWED | Posted: 15 November 2021 doi:10.20944/preprints202111.0262.v1

Now look at the impact of applied voltage on changes of P_{out} based on the structure of near-surface layer of a $LiNbO_3$ crystal. For the measurements of output optical power for applied voltage of 3 and 7 *V* see Fig. 3. Similar results are obtained across the measurement range of ±8 V. When voltage changes its polarity, voltage changes its sign to opposite one and remains unchanged until it is switched back. Therefore P_{out} is determined only by processes occurring in a waveguide itself at every moment, except for the moment of polarity changing.

When polarity changes, output optical power corresponding to the operating point position on the transfer function of EO-modulator changes abruptly (Fig. 4). However, the operating point moves to a position that does not correspond to the switching voltage. Accordingly, some relaxation time of the operating point is necessary to return to the required position. In fig. 4 shows a double voltage switching circuit. After first switching voltage (position 2, operating point was fixed during 5 min), and then was second switch of voltage and the operating point should return to the initial position -3 V. But operating point jump to position 3, which does not correspond -3V. There is a certain pattern that the operating point almost always goes further than necessary and then returns to initial position 1, which is clearly visible in Fig. 3.

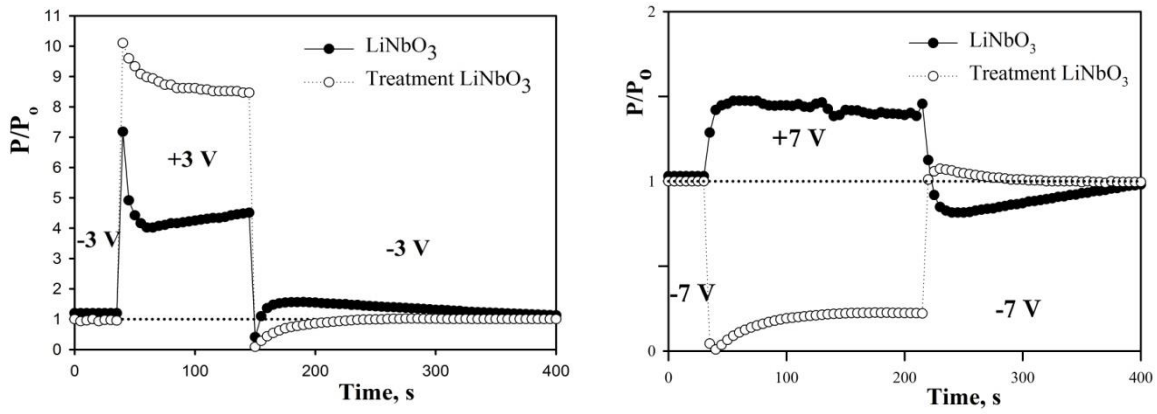

(**a**) (**b**)

Figure 3. Short-term DC-drift at ±3 (a) and ±7 V (b).

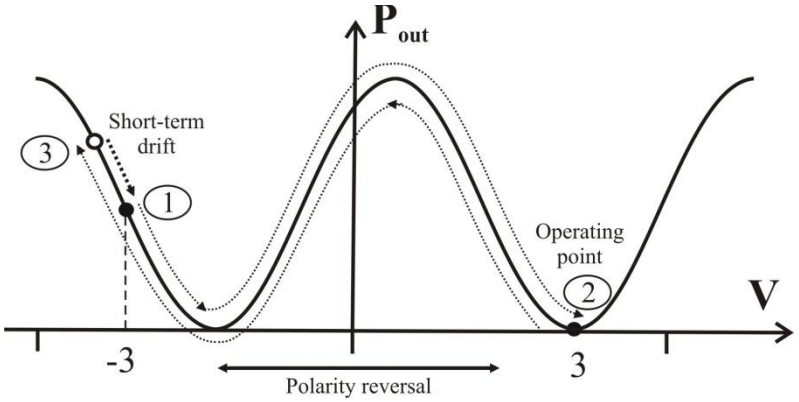

Figure 4. Mechanism of short-term DC-drift measurements.

Relaxation time of the output optical power to its initial value (variance is less than 1 percent) after double (– → + → –) switching, in our case, is a characteristic of a modulator showing how fast DC-drift becomes extinct. Extinction of DC-drift in EO-modulators after treatment $LiNbO_3$ is two times faster than extinction in reference samples: 116±22 seconds for annealed wafer samples and 286±37 seconds for reference samples. This significant difference in relaxation time of DC-drift is determined by homogeneous structure obtained after treatment of disturbed near-surface layer of $LiNbO_3$ crystal. The

Preprints (www.preprints.org) | NOT PEER-REVIEWED | Posted: 15 November 2021 doi:10.20944/preprints202111.0262.v1

treatment process eliminates internal strain (reduces microstrains), removes point defects and dislocations and improves the microstructure as shown in [16]. After treatment, once voltage V_{bias} is applied, it is much more difficult for charged defects to move, creating local electric fields in the area of APE waveguides, contributing to changes of refraction index and DC-drift. Thus, our test shows that the structure of the near-surface layer of a $LiNbO_3$ crystal affects drift parameters of EO-modulators through electro-optical effect and that the method of the layer treatment is effective for increasing stability of short-term DC-drift.

It is also important that operating point of EO-modulators without treatment structure of the near-surface layer of $LiNbO_3$ crystal is unstable after applied voltage V_{bias} changes its sign for the first period. This short-term drift in the first period will stabilize very quickly, since these are short-term drift processes associated with a change in the vector of the electric field strength and the movement of charged defects, which will come to equilibrium depending on the homogeneity of the structure around the waveguides. This is confirmed by long-term studies at room temperature (next section), when the optical power is practically unchanged. The activation energy of internal drift in EO-modulators is analyzed below.

We would like to note that our technique for studying the short-term drift of the operating point is important precisely from a scientific point of view for detection these rapid changes in EO-modulators.

3.2. Temperature stability of EO-modulators (long-term DC-drift)

In terms of device operation stability and reliability, it is necessary to know the value of activation energy E_a of DC-drift in EO-modulator. In our research, this parameter is a key to analysis of temperature impact on DC-drift. Previously, this analysis was performed in [6, 20] to evaluate the life cycle of EO-modulators based on $LiNbO_3$ X-cut. The experiment was performed at the following conditions. Operating point was fixed on a linear section of the transfer function at constant voltage $V_0 = 4.5\ V$. The experiment showed that as the temperature changes the operating point drifts and after some time achieves a new stable state (saturation). The P_{out} can be represented by the following power function:

$$P_{out}(t)/P_0 = A_0 \cdot t^n, \quad (3)$$

where A_0 – coefficient, P_0 – output optical power at V_0. Speed of DC-drift decreases as operating time of a device increases $\frac{dP_{out}(t)}{dt} \sim t^{n-1}$, therefore index n should be within the range $0 < n < 1$. At the same time, output optical power depends on temperature:

$$P_{out}(t,T)/P_0 = (B_0(T) \cdot t)^n, \quad (4)$$

where T – temperature, $B_0(T) \sim e^{\frac{-E_a}{kT}}$ – speed constant proportional to Arrhenius function. The equation (3) shows experimentally observed change of output optical power rather than the full physical nature of DC-drift. This profile can be used for comparative analysis of activation energy of DC-drift in EO-modulators with treatment structure of $LiNbO_3$ near-surface layer. Fig. 5 shows P_{out} dependency on time at various temperatures.

To determine E_a, first we normalized the test data according to equation (3) and then adjusted curves with the simplest (linear) equation to the obtained results (Fig. 5) to calculate coefficients A_0 and n. Using equations (3) and (4), we calculated the speed constant B_0. To build the Arrhenius function (Fig. 6), we used coefficient data (Table 2) at temperatures of 50-90 °C. From a slope of the plots, E_a was obtained. Activation energy of DC-drift for test samples after treatment and reference samples was 1.5 and 0.8 eV, respectively. The obtained values are not directly activation energy of the material, but relate to the entire test system according to the equation (3). However what's important for us is comparative analysis of DC-drift in EO-modulators after treatment $LiNbO_3$ structure obtained at identical process conditions and E_a calculations. Activation energy for treatment $LiNbO_3$ is about two times higher. To switch the entire system to unstable state, one should use two times more energy. In other words, the system stability

Preprints (www.preprints.org) | NOT PEER-REVIEWED | Posted: 15 November 2021 doi:10.20944/preprints202111.0262.v1

increases after treatment of $LiNbO_3$ structure – DC-drift decreases. This results from reduction of charged defects in the area of APE channel waveguides and $LiNbO_3$ near-surface layer which were described as the main source of DC-drift in EO-modulators in the previous section and in [15].

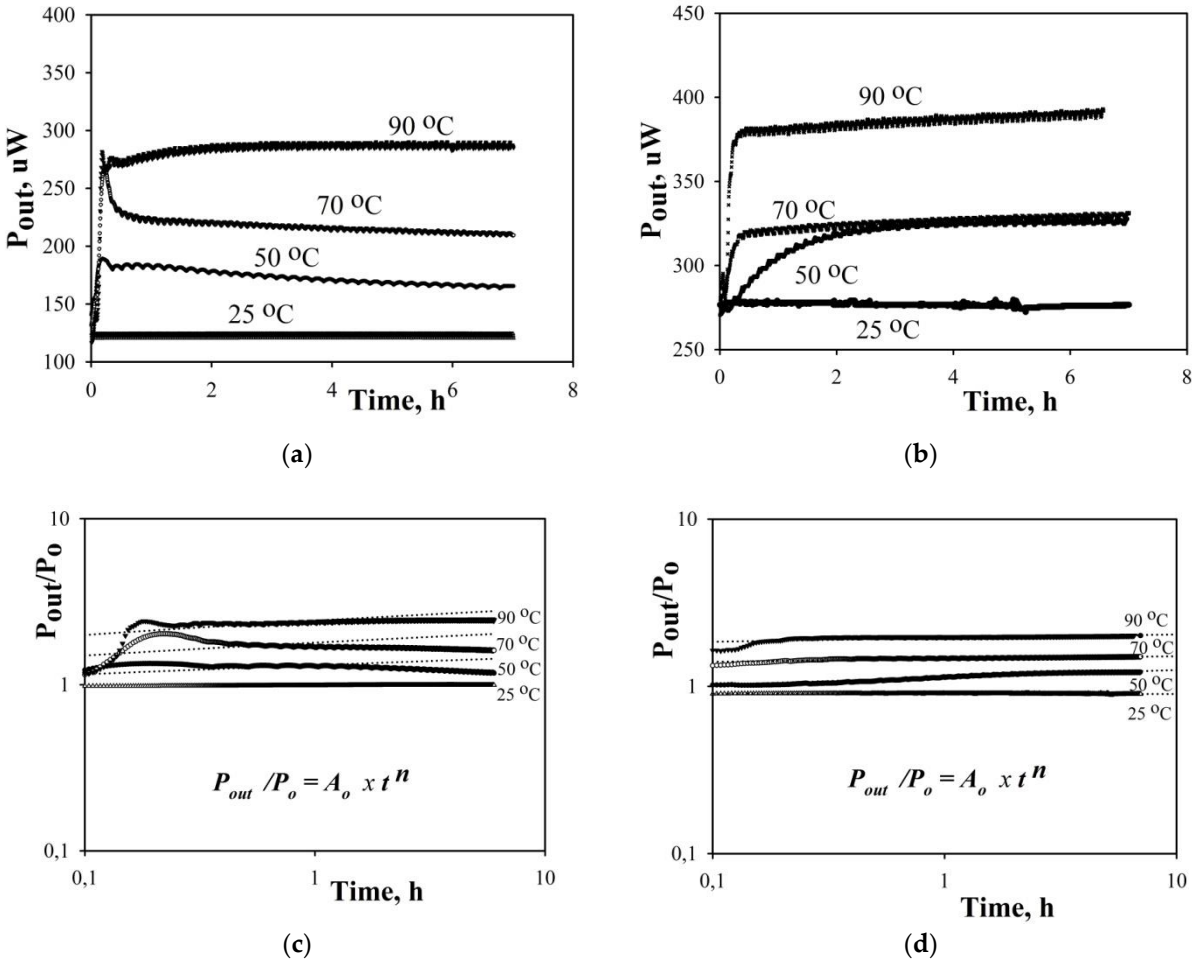

Figure 5. DC-drift curves measured on EO-modulators at 50, 70 and 90 °C: reference (a, c) and after treatment $LiNbO_3$ (b, d). Plots (c) and (d) is replots of (a) and (b).

In paper [6], obtained values of activation energy of DC-drift (0.7, 1.0 and 1.2 eV) were used to evaluate the number of failures occurred during operation of EO-modulators over 20 years. The number of failures at 50 °C was 3 errors with $E_a = 1.2$ eV, 25 errors with $E_a = 1.0$ eV and 260 errors with $E_a = 0.7$ eV. Therefore, the higher the activation energy of DC-drift the better the stability of the entire device, resulting in a smaller number of errors during long-time operation of EO-modulators. The obtained comparative results $E_{a1}/E_{a2} = 1.8$, where E_{a1} – activation energy of a modulator after treatment $LiNbO_3$ and E_{a2} – activation energy of a references modulator enables us to draw a firm conclusion that $LiNbO_3$-based EO-modulators can operate longer with a smaller number of errors at the defined driver parameters after treatment near-surface structure.

Table 2. Calculated parameters on DC-drift of EO-modulators

Sample	Temperature, °C	Coefficient, A_0	Coefficient, n	Coefficient, B_0 [1/h]
$LiNbO_3$	25	0.984	0.003	0.0046
	50	0.842	0.068	0.079
	70	0.909	0.128	0.475
	90	1.112	0.191	1.745

Preprints (www.preprints.org) | NOT PEER-REVIEWED | Posted: 15 November 2021 doi:10.20944/preprints202111.0262.v1

	25	0.981	0.002	0.00004
Treatment	50	0.783	0.051	0.008
$LiNbO_3$	70	0.992	0.024	0.708
	90	1.050	0.043	3.180

Reported E_a varies between 1.0 eV and 1.4 eV for unbuffered X-cut $LiNbO_3$ [21,22]. This range of activation energies means a broad range of acceleration factors. Our result with E_a = 1.6 eV agrees quite accurately with these data and demonstrates the reliable long-term behavior of EO-modulators after treatment.

Thus the temperature tests showed significant improvement in drift parameters of EO-modulators after treatment $LiNbO_3$ structure. Our idea of improving the operation stability of EO-modulators by monitoring material parameters of the transfer function has proved its effectiveness at various experimental conditions and can be applied to systems based on other optical materials.

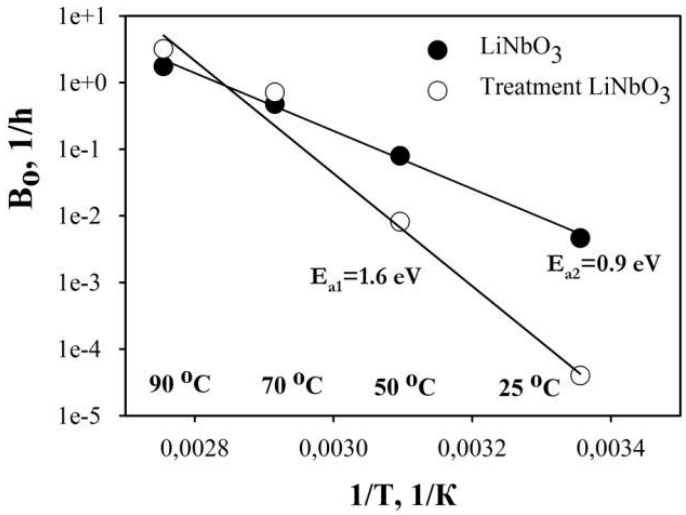

Figure 6. Arrhenius plots of experimental EO-modulators.

5. Conclusions

This work was focused on testing the impact of material parameters of the transfer function (defective microstructure of near-surface layer of a $LiNbO_3$ crystal) on the stability of EO-modulator characteristics. We performed a comprehensive analysis of the effect of $LiNbO_3$ microstructure treatment on the level of DC-drift in EO-modulators, enabling us to draw the following conclusions:

- Relaxation time of short-term drift of operating point decreases from 286 to 116 seconds;
- Activation energy of operating point in EO-modulators showed grows from 0.9 to 1.6 eV.

Thus, EO-modulators demonstrated more stable state of the system in general. All results obtained in this work support each other, demonstrating the impact of material factors of the transfer function on DC-drift in EO-modulators. Our method of treatment the structure of disturbed near-surface layer of a $LiNbO_3$ crystal proved its effectiveness for reducing short and long-term drifts in EO-modulators.

Author Contributions: Conceptualization and drift experiments, A.S.; methodology and writing, R.P.; formal analysis and optic measurements, A.Z.; resources and creation samples, S.M. and M.K. All authors have read and agreed to the published version of the manuscript.

Funding: This research was funded by RFBR and Perm Territory, project number 20-42-596001 (samples study) and Ministry of Education and Science of Perm region under Contract No. C-26/848 (samples design).

Conflicts of Interest: The authors declare no conflict of interest.

References

1. Noguchi, K. Lithium Niobate Modulators, in Broadband optical modulators: science, technology, and applications, ed. Chen A., Murphy E. J. Boca Raton: CRC Press, 2012, pp. 151-172.
2. Rao, A.; Fathpour, S. Compact Lithium Niobate Electrooptic Modulators. *IEEE J. Sel. Top. Quantum Electron*. **2018**, *24*, 1-14.
3. Han H.; Xiang, B. Integrated electro-optic modulators in x-cut lithium niobate thin film. *Optik*. **2020**, *212*, 164691.
4. Wooten, E.L. et al. Review of lithium niobate modulators for fiber-optic communications systems. *IEEE J. Sel. Top. Quantum Electron*. **2000**, *6*, 69-82.
5. Nagata, H. Long-term DC drift in x-cut $LiNbO_3$ modulators without oxide buffer layer. *IEE Proc.-Optoelectronics*. **2000**, *147*, 350-354.
6. Nagata, H.; Papasavvas, N. Bias stability of OC48 x-cut lithium-niobate optical modulators: four years of biased aging test results. *IEEE Technol. Lett.* **2003**, *15*, 42-44.
7. Hofer, L.R. et al. Bias Voltage Control in Pulsed Applications for Mach-Zehnder Electrooptic Intensity Modulators. *IEEE Trans. Control Syst. Technol.* **2017**, *25*, 1890-1895.
8. Yuan, X. et al. Any point bias control technique for MZ modulator. *Optik.* **2019**, *178*, 918-922.
9. Svarny, J. Analysis of quadrature bias-point drift of Mach-Zehnder electro-optic modulator. *Proc. 12th Biennial Baltic Electronics Conference*. **2010**, 231-234.
10. Cho, P.S.; Khurgin, J.B.; Shpantzer, I. Closed-Loop Bias Control of Optical Quadrature Modulator. *IEEE Photonic Technol. Lett.* **2006**, *18*, 2209-2211.
11. Wang, L.L.; Kowalcyzk, T.A. Versatile Bias Control Technique for Any-Point Locking in Lithium Niobate Mach-Zehnder Modulators. *J. Lightwave Tech.* **2010**, *28*, 1703-1706.
12. Toney, J.E.; Stenger, V.E.; Pollick, A.; Sriram, S. Operating Point Correction for Mach Zehnder Interferometer-based Electro-optic E-field Sensors. *Proc. Optical Sensors and Sensing Congress (ES, FTS, HISE, Sensors)*. **2019**, SW4C.1.
13. Bui, D.T. et. al. Instrumentation system for determination and compensation of electro-optic modulator transfer function drift, *Measurement Science and Technol.* **2011**, *22*, 125105.
14. Fu, Y. et. al. Mach-Zehnder: A Review of Bias Control Techniques for Mach-Zehnder Modulators in Photonic Analog Links, *IEEE Microwave magazine*. **2013**, *14*, 102-107.
15. Salvestrini, J.P. et. al. Analysis and Control of the DC Drift in $LiNbO_3$-Based Mach-Zehnder Modulators. *J. Lightwave Technol.* **2011**, *29*, 1522-1534.
16. Sosunov, A.V. et. al. Effect of the structure and mechanical properties of the near-surface layer of lithium niobate single crystals on the manufacture of integrated optic circuits. *Optoelectronics, Instrumentation and Data Processing*. **2017**, *53*, 82-87.
17. Piecha, J. et al. Features of surface layer of $LiNbO_3$ as-received single crystals: Studied in situ on treatment samples modified by elevated temperature. *Solid State Ionics.* **2016**, *290*, 31-39.
18. Sosunov, A. et. al. Effect of pre-annealing of lithium niobate on the structure and optical characteristics of proton-exchanged waveguides. *Optical Materials.* **2019**, *88*, 176-180.
19. Suchoski, P.G.; Findakly, T.K.; Leonberger, F.J. Stable low-loss proton-exchanged $LiNbO_3$ waveguide devices with no electro-optic degradation. *Opt. Lett.* **1988**, *13*, 1050-1052.
20. Nagata, H. Activation Energy of DC-Drift of X-Cut $LiNbO_3$. *IEEE Photonic Technol. Lett.* **2000**, *12*, 386-388.
21. Nagata, H.; Li, Y.; Croston, I.; Maack, D.R. and Appleyard, A. Dc drift activation energy of $LiNbO_3$ optical modulators based on thousands of hours of active accelerated aging tests. *IEEE Photon. Technol. Lett.* **2002**, *14*, 1076-1078.
22. Nagata, H.; Ishizuka, Y. and Akizuki, K. Temperature dependency of X-cut $LiNbO_3$ modulator dc drift. *Electron. Lett.* **2000**, *36*, 1952-1953.

Preprints (www.preprints.org) | NOT PEER-REVIEWED | Posted: 15 November 2021 doi:10.20944/preprints202111.0262.v1

Response to Reviewer

1. **Line 93, "After drying and development of the photoresist the remaining Al_2O_3 protective film was removed...". It seems that the etching step after development was left out? Please carefully check the fabrication part**

Response 1. Yes, we add etching step in section 2.1:
After drying and development of the photoresist, its active part was removed in organic solvent. Then, Al_2O_3 protective film was etched using nitric acid solution and removed remains of photoresist. 6 um wide channels were created.

2. **Figure 2, why are the electrodes for building EO modulator placed asymmetrically?**

Response 2. No, electrodes were symmetrical. Fig. 2 (now Fig. 1) was fixed.

3. **Will this method influence the performance of the EO modulator? The comparison between the modulator before and after treatment should be provided, for example, the half-wave voltage and modulation speed**

Treatment of $LiNbO_3$ directly affects the optical characteristics of APE channel waveguides with identical formation technology. In particular, defects and internal stresses in the near-surface layer of $LiNbO_3$ can increase the light scattering passing through optical channel waveguides. Moreover, any defects in the region of the waveguides obtained by ion exchange methods deteriorate the polarizing properties of the waveguide, which leads to decrease in the extinction of the EO-modulator (added in section 2.1). However, the half-wave voltage depends largely on the design of the modulator itself.

4. **Figure 5(c), the equation was written with errors, please carefully check.**

Response 4. Fig. 5c and Fig. 5d are made using the one method. Experimental data (solid lines) were approximated by $P/P_0=k*Ln(t)+b$ – linear function in logarithmic scale. The results are presented in fixed and improved form (Fig. 5).

5. **Figure 5, did the authors use the same P0 for the reference and after treatment LiNbO3? Obviously, the stable Pout for after treatment LiNbO3 is around 400 μW, larger than the reference LiNbO3. However, in (c), the Pout/P0 of the reference LiNbO3 is larger than that of after treatment LiNbO3. What causes these differences?**

Response 5. The optical power P_0 corresponds to the value of the applied voltage V_0 = 4.5 V for each modulator. These values are different, because transfer functions and half-wave voltages are different for each modulator.
Fig. 5 c,d these are replots Fig. 5 a,b in a logarithmic scale without any changes. The increase in optical power in Fig. 5c after normalization is due to the difference between the minimum and maximum values. This demonstrates the easy activation of defects with increasing temperature.

6. **Referring to Eq. (4), $B_0(T)\sim e^{\frac{-E_a}{kT}}$, why did the authors use the linear fitting in Fig. 6? The fitting result for after treatment LiNbO3 is not good**

Response 6. In fig. 6 is not a linear function, but an exponential function, built on a logarithmic scale. The drift rate is proportional to the Arrhenius function, and the activation energy can be calculated by taking the logarithm of both sides of the equation $B_0(T)\sim e^{\frac{-E_a}{kT}}$, and constructing a linear graph.

We added room temperature to increase the amount of data, but at higher temperatures (above 100 °C) we cannot investigate modulators because this was originally a manufacturer's recommendation. Therefore, such a temperature range was chosen.

Preprints (www.preprints.org) | NOT PEER-REVIEWED | Posted: 15 November 2021 doi:10.20944/preprints202111.0262.v1

Now the fitting curves fit well the experimental points and the activation energy changes slightly accordingly (Ea1=1.6 eV, Ea2=0.9 eV), since the slope of the Arrhenius curve changes.
This method primarily allows for a qualitative comparison of EO-modulators with and without lithium niobate treatment.

7. **Will this method suitable for the EO modulator based on a Lithium-Niobate-on-Insulator platform**

Response 7. Surface and near-surface characteristics can affect roughness of the sidewall of the ridge waveguides and the photolithographic mask. In this case, yes, our method allows for better results for LN-on-insulator.

8. **The experiment part of the manuscript can be more organized if the experimental results are provided immediately after the description of the experiment details**

Response 8. We agree that this may be somewhat more convenient, but we adhere to the structure of the article, which recommended by the editorial board of the journal.

9. **In Fig. 4, the manuscript lacks the result of P/P0 of the lithium niobate without treatment in the first periods when the first voltages were applied**

Response 9. The voltage using a continuous adjusting resistor manually was changed. After that, the polarity at a fixed voltage was changed to study the short-term drift (added in section 2.3).
We think, that the reviewer did not see the black dots P/P0 at the first period, because they are behind white points. Of course, they are also there result of P/P0 of the lithium niobate without treatment in the first periods.
Fig. 4 (now fig. 3) was fixed, to show results P/P0 at the first period.

10. **In Fig. 4a, when the voltage changes from -3 to +3 V, the LiNbO3 without treatment seems to increase after decreasing first, and then the voltage changes to -3 V again. What if the voltage keeps +3 V, will the P/P_0 be stable or will it keep on increasing? This question can also be applied to other cases in Fig. 4.**

Response 10. Of course, the position of the operating point stabilizes at some short time at +3 V, by analogy with our analysis for -3 V. We investigated this short-term instability. Voltage polarity reversals can be performed repeatedly and the relaxation time of the operating point drift can be analyzed.
This short-term drift in the first period will stabilize very quickly, since these are short-term drift processes associated with a change in the vector of the electric field strength and the movement of charged defects, which will come to equilibrium depending on the homogeneity of the structure around the waveguides. This is confirmed by long-term studies at room temperature (next section), when the optical power is practically unchanged.
We have added an explanatory Fig. 4 and its description for short-term drift in section 3.1.

11. **The case for room temperature should be added to the temperature experiments**

Response 11. Experimental results of room temperature were added in Fig. 5. Now the fitting curves fit well the experimental points and the activation energy changes slightly accordingly (Ea1=1.6 eV, Ea2=0.9 eV), since the slope of the Arrhenius curve changes.